HEAT TRANSFER IN TWO-PHASE IMPINGING JETS

K. Cannevière and J. Réveillon*
LMFN / CORIA UMR CNRS 6614
University of Rouen
INSA, Avenue de l'université
76800 Saint Etienne du Rouvray, France

C. Canton-Desmeuzes
CEA/CESTA
Groupe Rentrée Etudes et Conception
CESTA B.P.2
33114 Le Barp, France

ABSTRACT

This work is dedicated to the study of the heat transfer rates within an impinging jet transporting solid particles. Two main configurations have been studied thanks to direct numerical simulations. First, injection and mixing of a spray injected within the main flow was computed. The particles modify strongly the turbulence properties. Consequently, heat transfers between the flow and the impacted wall are strongly modified compared to a one-phase jet impingement. In the second configuration, few solid particles hit the wall and induce the emission of ejecta which are scattered in the turbulent boundary layer and modify again the heat transfers at the wall. It is shown that these two situations alter heat transfers but in an entirely different way. Indeed, particles embedded in the turbulence increase heat transfers whereas ejecta tend to decrease it, compared to a one-phase situation.

INTRODUCTION

High speed reentry bodies often cross clouds composed of solid (ice) or liquid (droplets) particles of water. The impact of these particles on the flying body leads to the apparition of ejecta (or micro-particles of carbon) due to multiple micro-perforations of the external surface.

Experiments (Desmeuzes 1997) showed that the presence of these ejecta near the wall modifies in a significant way the heat transfers between the turbulent atmosphere and the solid surface.

In the case of a purely gaseous flow, it is known (Van Fossen *et al* 1995) that several criteria affect the heat transfer with the wall (turbulence intensity, Reynolds number, shape of the impacted surface, ...). In a general way, in the area of the stagnation point (intersection between the wall and the axis of symmetry where the spanwise component of the mean velocity is null), the more the intensity of turbulence is strong, the more the heat transfer is significant. Moreover, it was shown (Kaftori *et al* 1998, Wells and Stock 1983, Hestroni 1989) that the presence of particles in a turbulent flow can strongly modify (positively or negatively) the intensity of turbulence according to their mass, size and concentration.

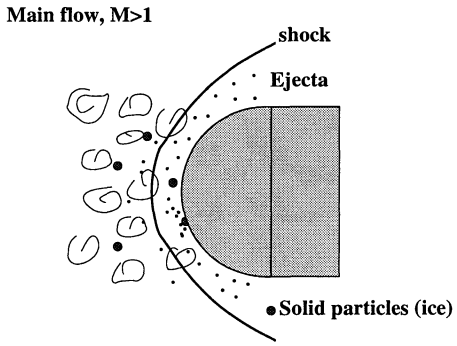

FIG. 1 – **General sketch of a flying body**

The objective of this work is to study the effect of the ejecta issued from the solid surface on heat transfers. To this end, a two-way coupled Eulerian-Lagrangian formulation (Squires and Eaton 1990) has been used to describe the turbulent flow and the dispersion of the particles. Direct numerical simulation (DNS) of the gas phase coupled with a Lagrangian solver to describe the dispersed phase gave access to the whole physical parameters. Therefore,

*Corresponding author - reveillon@coria.fr

a detailed study of turbulence properties and heat transfers close to the wall have been completed.

NUMERICAL PROCEDURE

In the Lagrangian view adopted for the spray, the properties of each droplet are estimated by solving a system of two equations. This system may be written for the position X_i and the velocity V_i of each droplet as:

$$\begin{aligned} \frac{\mathrm{d}X_i}{\mathrm{d}t} &= V_i \\ \frac{\mathrm{d}\left(\Theta\right)^3 V_i}{\mathrm{d}t} &= AD_i \end{aligned}$$

with the drag force given by:

$$D_i = \rho\frac{\pi}{8}\Theta^2 C_D \left|\underline{U} - \underline{V}\right| \left(U_i - V_i\right)$$

In the above equation, C_D is the drag force coefficient, defined by

$$C_D = \frac{24}{Re_D}\left(1 + \frac{{Re_D}^{2/3}}{6}\right)$$

$Re_D = \left|\underline{U} - \underline{V}\right| \Theta/\nu$ is the particle Reynolds number and $A = 6/\left(\pi\rho_p\right)$, is a constant parameter in which ρ_p is the solid-phase constant density. The properties of the gas ($\mu = \rho\nu$ viscosity, ρ density and U_i velocity) are obtained at the droplet position from the grid nodes using a third order interpolation algorithm. These equations have been made dimensionless, with R_e as the acoustic Reynolds number of the DNS problem,

The flow is described in the Eulerian context by the following equations accounting for the two-way coupling:

$$\begin{aligned} \frac{D\,\rho}{D\,t} &= 0 \\ \frac{D\,\rho U_i}{D\,t} &= -\frac{\partial P}{\partial x_i} + \frac{1}{R_e}\frac{\partial \sigma_{ij}}{\partial x_j} - \frac{1}{\mathcal{V}}\sum_k D_i^k \\ \frac{D\,\rho E_t}{D\,t} + \frac{\partial P U_j}{\partial x_j} &= \frac{\partial}{\partial x_i}\left(\frac{\mu C_p}{R_e Pr}\frac{\partial T}{\partial x_i}\right) \\ &\quad + \frac{1}{R_e}\frac{\partial \sigma_{ij} U_j}{\partial x_i} - \frac{1}{\mathcal{V}}\sum_k V_i^k D_i^k \end{aligned}$$

where

$$\frac{D\,(*)}{D\,t} = \frac{\partial(*)}{\partial t} + \frac{\partial(*)U_j}{\partial x_j}$$

To achieve the coupling between the Eulerian and Lagrangian description, the source term of momentum of each droplet is accumulated in a volume $\mathcal{V}$ defined in the vicinity of the Eulerian grid point.

A third order Runge-Kutta scheme with a minimal data storage method (Wray 1990) is used for time stepping. Spatial derivatives are estimated using a sixth order PADE scheme (Lele 1992).

COMPUTATIONAL CONFIGURATION

To be able to use a DNS solver, the geometry of the reentry vehicle was simplified. An impinging turbulent jet configuration has been chosen so that the basic physical phenomena we are interested in may be studied. Indeed, this Cartesian configuration allows us to describe the turbulence/particles/wall interactions in a simple way. Thus, a first sight of the physics of particles impacts and ejecta generation will be offered.

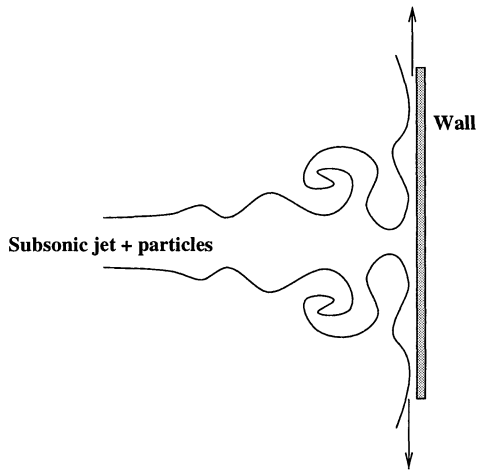

FIG. 2 – **Sketch of the simulated configuration**

The figure 2 shows a sketch of the configuration. A weak coflow is injected along with the jet, the amplitude of which follows sinusoidal anti-symmetric oscillations. The oscillation period is based on the Strouhal number which has been set to 0.4 according to the optimal destabilization frequency of the jet. This procedure makes it possible to generate turbulent structures quickly so that the flow is fully turbulent when it reaches the wall.

All the simulations are carried out with exactly the same initial and boundary conditions for the gas flow. Moreover, the computational domain remains the same. Only the dispersed phase parameters are varying in the various simulations. So, variations of results are strictly due to the solid phase dispersion.

Simulation	Ejecta	$\frac{\Sigma E_e}{E_i}$	$\frac{\Sigma M_e}{M_i}$	Θ_e	Θ_i
BASE	No	-	-		
Y15-N15	No	-	-	-	0.009
Y15-N30	No	-	-	-	0.0045
Y25-N15	No	-	-	-	0.01
Y25-N30	No	-	-	-	0.0053
E1-M10	Yes	1.	10.	0.006	0.01
E1-M5	Yes	1.	5.	0.006	0.01
E66-M10	Yes	0.66	10.	0.006	0.01
E66-M5	Yes	0.66	5.	0.006	0.01

TAB. 1 – *Simulation parameters. The BASE case is a one-phase simulation used as reference flow. The Y* set corresponds to the single impact procedure. $Y25 - N15$ gives the following informations: ranks of 15 particles of ice (N15) are injected in the jet width, the frequency of injection being determined by the water mass fraction in the jet width: Y=25/100 (Y25). The E* set correspond to the impact with ejecta procedure. ΣM_e and ΣE_e are the total mass and total kinetic energy of the ejecta emitted after the impact of one particle of ice. The mass and the kinetic energy of this particle are M_i and E_i. Θ_e and Θ_i are the ice and ejecta diameters.*

Two distinct configurations were considered. First, many particles are injected along with the jet in the computational domain. Particles are mixed by the turbulent flow before impacting on the wall where a reflection boundary condition is carried out. The angle of reflection r is equal and symmetric to the angle of incidence i (fig. 3). However, the kinetic energy of the particle before (E_i) and after (E_r) the impact may differ (Table 1). In a second set of simulations, few particles are injected along with the jet. They barely modify the turbulent flow before impacting the wall. Then, ejecta are issued from the impingement. These new particles are smaller but numerous. Their mass (M_e) and kinetic energy are detailed table 1. Ejecta are emitted without any privileged direction. Thus, the angle between the direction perpendicular to the wall and the ejecta trajectory is randomly determined in the following range: $[-\pi/2, \pi/2]$. When an ejectum reaches the wall again, the processing of the impact is carried out according to the first procedure. Figure 3 shows sketches of the two procedures.

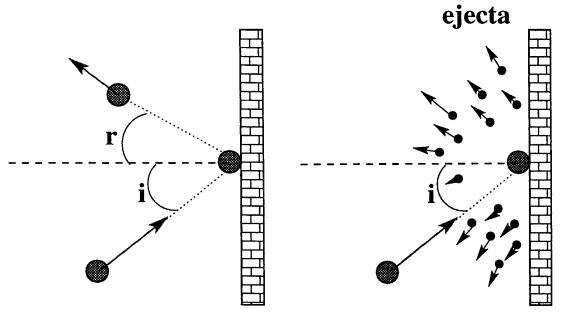

FIG. 3 – *Sketches of the single reflection procedure (left) and of the emission of ejecta procedure (right)*

All the results presented in this work are dimensionless. The reference parameters are the following: u_0 is the maximum jet velocity, t_0 is the time period of the jet perturbations. It was chosen to obtain an optimal Strouhal number equal to 0.4. Then, $l_0 = u_0 * t_0$, is our reference length. Therefore, the jet width is 0.4, the inlet/wall distance is equal to 4 and the width of the computational domain is equal to 2.

The computational grid ($321 * 192$ nodes) is uniform along the spanwise direction (y). Along the streamwise (x) direction, the mesh spacing is strongly reduced close to the wall to take into account the boundary layer of the flow.

RESULTS

The main objective of this work is to study the effect of turbulence on heat transfers between some two-phase flows and a wall. To begin with, a reference simulation (BASE) has been carried out. This purely gaseous flow allowed us to quantify heat transfers without any modification of the turbulence by a dispersed phase.

As described above, two sets of simulation were carried out. For the first one (Y*, see table 1), four simulations were carried out with many ice particles impacting the wall without generating ejecta. For the second set (E*), few particles of ice produce ejecta. Results show that the general properties of the flow within a same family are similar even if their orders of magnitude vary according to the dispersed phase properties. Therefore, within the framework of this paper, only a comparison between these two sets of simulation (with or without ejecta) will be carried out. It will be shown that the differences are significant.

'BASE' simulation

The jet destabilization is due to the strong velocity gradients and to the prescribed anti-symmetrical oscillations of its amplitude. Figure 4-(a) shows the formation and the evolution of the turbulent structures.

The anti-symmetric oscillations generate turbulent structures very quickly and the destabilization of the jet takes place at a short distance (0.2, that is half the injection width) of the injection. The anti-symmetry has a repercussion on the position of the turbulent structures which hit the wall alternately (fig. 4-(a)). Nevertheless, the evolution of the time averaged parameters is similar around the axis ($y = 1$) of injection. Thus, this method enables us to gather a statistical sampling twice more significant than symmetric oscillations would have

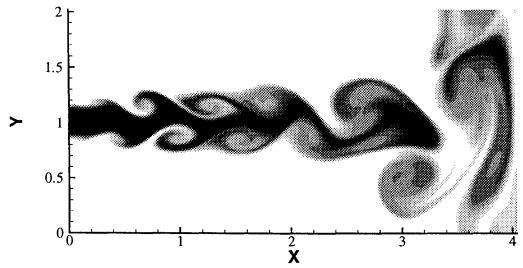

(a) *Inert scalar topology*

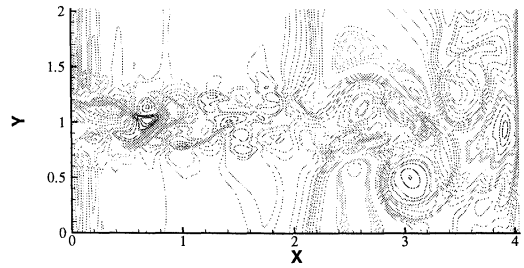

(b) *Temperature fluctuations*

FIG. 4 – *Effect of the turbulent vortices on (a) an inert scalar injected along with the jet and (b) on the temperature field.*

provided us. The instantaneous field of temperature at the moment $t = 15.4$ (fig. 4-(b)) shows the apparition of fluctuations of temperature. These fluctuations are generated naturally by the turbulent structures but also by the prescribed velocity oscillations at the inlet. However, these last fluctuations of temperature are weak and are dissipated quickly. On the other hand, close to the wall, the vortices are now fully developed, and significant fluctuations of temperature are present. They have a great effect on the heat transfer between the flow and the wall. The figure 5 shows the detail of the impact of a turbulent structure on the wall. The crushing of the vortices induces a strong variation of the temperature fluctuations, which in a general way, will increase.

The computation of the time averaged heat fluxes $H_w(y) = \left\langle -\lambda \left(\frac{\partial T}{\partial x_i} \right)_w \right\rangle$ between the flow and the wall shows a regular curve (fig. 6), the maximum of which is located at the point of stagnation of the flow (y=1). The objective of this work is to evaluate the effects of a dispersed phase embedded in the jet. Therefore, the heat transfer rate at the point of stagnation of the flow (H_{w0}) has been used as reference value. Our interest is to be able to compare the heat transfer fluctuations around this reference value according to the general parameters of the dispersed phase.

'Two-phase' simulations

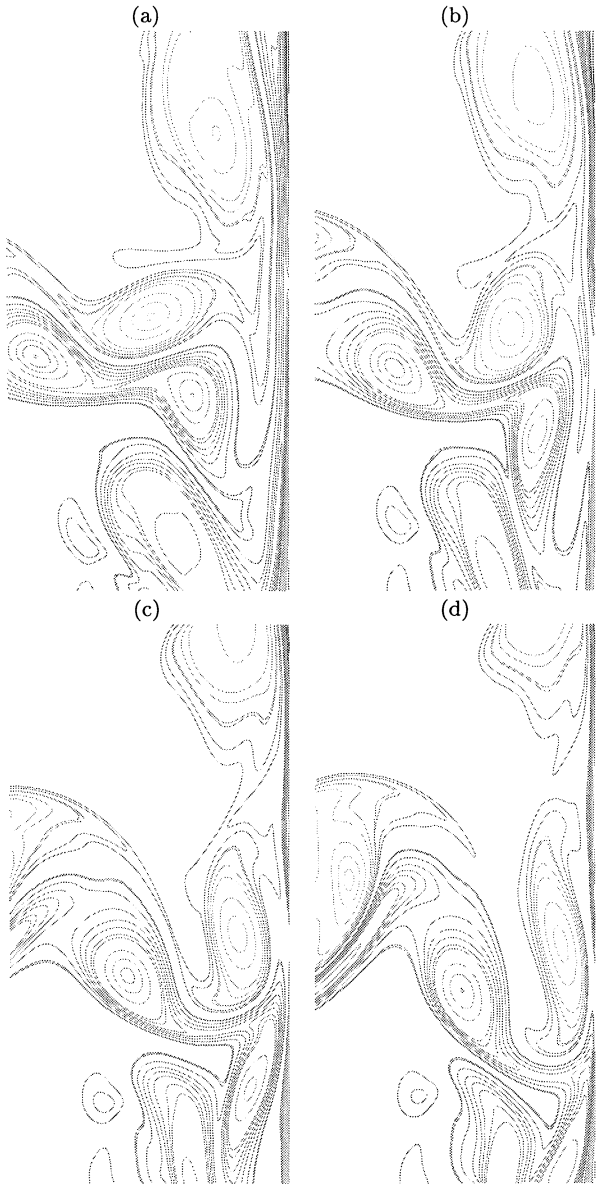

FIG. 5 – *Detail of the impact of a vortex. (a) $t = 8.7$, (b) $t = 10.6$, (c) $t = 12.5$, (d) $t = 14.4$*

Simulations, identical from the point of view of the boundary conditions to the reference computation 'BASE', have been carried out following the parameters shown table 1. The statistics are determined on the same time interval. The figure 7 shows the iso-vorticity field of a complete E* configuration (see table 1) along with ice particles and ejecta. In spite of their significant initial kinetic energy, ejecta remain in the vicinity of the turbulent boundary layer. This figure shows in the same way the effect of the turbulent structures on the dispersion of the ice particles. The latters are ejected from the areas with strong vorticity. They may be seen (fig. 7) along the stagnation line ($y = y_s = 1.$) or outside the jet expansion area.

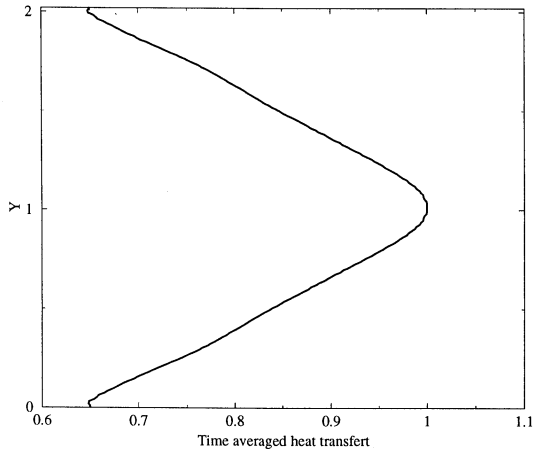

FIG. 6 – **Time averaged heat transfer $\langle H_w \rangle$ between the flow and the wall. The maximum value at the stagnation point is used as reference value.**

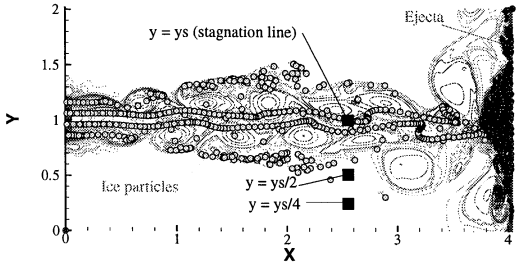

FIG. 7 – **Two-phase simulation. Large circles: ice particles, dots: ejecta, lines: iso-vorticity, squares: spanwise position of the measurements**

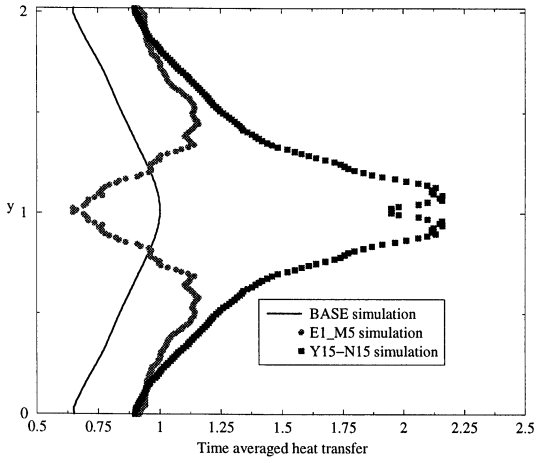

FIG. 8 – **Time averaged heat transfer $\langle H_w \rangle$ between the flow and the wall**

The main result of this study can be seen on the figure 8. It shows the temporal average of the heat transfer for each of the three main configurations: without particle, with particles without ejectum and finally with ejecta. As it has already been demonstrated in a preceding work (Kaftori *et al* 1998), an impinging jet whose turbulence is strongly modified by the

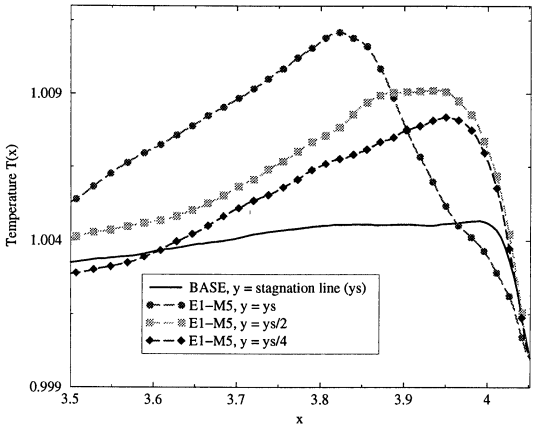

FIG. 9 – **Temperature profile near the wall along the streamwise direction. Line: one-phase flow profile along the stagnation line; symbols: simulation with ejecta. The profile line positions are shown figure 7**

presence of particles increases the heat transfers much more significantly than in the one-phase case. In our study, fluxes have increased by more than 100 percent.

The interesting element of this figure (fig. 8) is the shape of the heat transfer when ejecta are emitted. Indeed, one may notice a strong diminution of the heat transfer around the stagnation point. In this case, there are very few ice particles and they hardly modify the flow upstream. However, when ejecta are sent counterflow with a very strong kinetic energy, an important reduction of the heat transfer takes place. This phenomenon can be explained by the fact that the slip velocity of the particles (differential velocity between the particles and the flow) is very significant when they leave the wall. It generates, through the drag force, a strong increase of the turbulence intensity in the area where the temperature gradients are the most significant. Then, turbulent mixing decreases the gradients and thus heat transfers. Figure 9 shows the gradients diminution along the stagnation line. It also shows a large increase of the temperature level but far from the wall because turbulent mixing is prevalent.

Nevertheless, ejecta have very weak inertia and they follow very quickly the motion of the flow. Then, they have a more conventional behavior within the turbulent boundary layer. This is why, at a distance rather far away from the point of stagnation, heat transfers increase again to reach a level equivalent (fig. 8) to the two-phase case without generation of ejecta (Y15-N15). In this area, temperature gradients (fig. 9) are again more significant than in the one-phase 'BASE' case.

Figure 10 shows the effect of particles on the

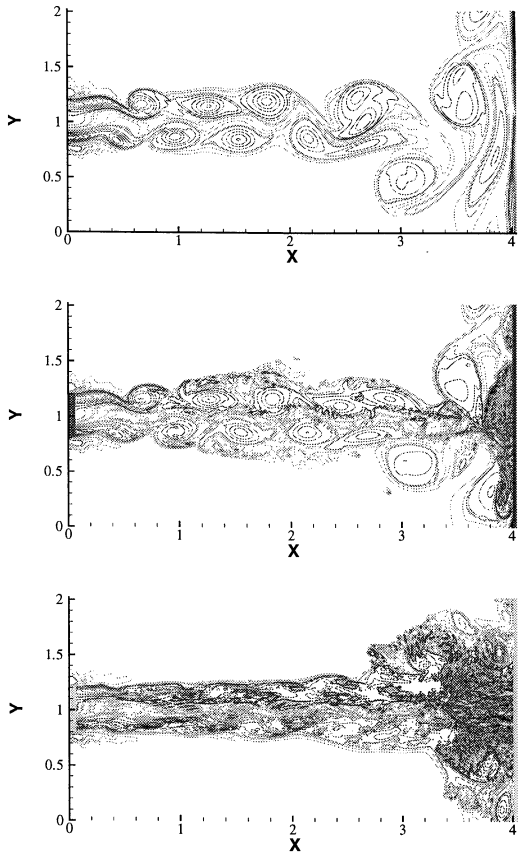

FIG. 10 – *Instantaneous vorticity field, same time $t = 15.5$. Top: BASE simulation (no particles), Middle: E1-M5 simulation (ice+ejecta), Bottom: Y15N15 simulation (many particles, no ejectum)*

vorticity field. Many small structures are generated in the wake of the clusters of particles. If the effect is not predominant in the upstream flow of the E1-M5 simulation, it is not true for the case Y15-N15. Moreover, the case E1-M5 shows, near the wall, the significant effects of ejecta on the flow.

CONCLUSION

It was shown in this paper that a dispersed solid phase embedded in a turbulent flow could significantly modify heat transfers between the fluid and the wall. The dispersion of the particles induces several effects. On the one hand we observed a strong increase of the intensity of the turbulence upstream of the impingement area. It generates significant heat transfers when the structures hit the wall. In addition, the presence of ejecta in the vicinity of the wall decreases heat transfers near the point of stagnation because of a strong turbulent mixing generated during the emission of ejecta. Nevertheless, when the slip velocity of ejecta decreases, in the boundary layer along the wall, heat transfers increase again in a consequent way.

ACKNOWLEDGMENTS

The authors wish to aknowledge the 'Commissariat à l'énergie atomique - C.E.A.' for its support of this work.

REFERENCES

Desmeuzes, C. (1997). Hydroérosion: Essai soufflerie, premiers dépouillement des essais onera diphasiques. Technical report, CEA/CESTA DIA/SCDA/GREC DO 256.

Van Fossen, G. J. V., Simoneau, R. J., and Ching, C. (1995). Influence of turbulence parameters,reynolds number, and body shape on stagnation-region heat transfer. *Journal of heat transfer*, 117(3):597–203.

Hestroni, G. (1989). Particle-turbulence interaction. *Int. J. Multiphase Flow*, 15(5):735–746.

Kaftori, D., Hestroni, G., and Banerjee, S. (1998). The effect of particles on wall turbulence. *Int. J. Multiphase Flow*, 24(3):359–386.

Lele, S. K. (1992). Compact finite difference schemes with spectral like resolution. *J. Comput. Phys.*, (103):16–42.

Squires, K. D. and Eaton, J. (1990). Measurements of particle dispersion obtained from direct numerical simulations of isotropic turbulence. *J. Fluid Mech.*, 226:1–35.

Wells, M. R. . and Stock, D. E. (1983). The effects of crossing trajectories on the dispersion of particles in a turbulent flow. *Journal of fluids mechanics*, 136:31–62.

Wray, A. A. (1990). Minimal storage time-advancement schemes for spectral methods. Technical report, Center for turbulence research Report, Stanford University.